Second Order Spectral Simulation of Directional Wave Generation and Propagation in a 3D Tank*

David Le Touzé, Félicien Bonnefoy & Pierre Ferrant

Division Hydrodynamique Navale/LMF, Ecole Centrale de Nantes, B.P. 92101, F-44321 Nantes Cedex 3, France
e-mail: pierre.ferrant@ec-nantes.fr

Abstract

This paper is devoted to the time accurate simulation of the generation and propagation of waves generated by a segmented wave maker in a 3D tank. The flow is described in the framework of potential theory, with second order Stokes expansion of nonlinear boundary conditions on the free surface and on the wave maker. The resulting initial boundary value problem is solved using a recently developed spectral formulation. The basic principles of the numerical scheme are first presented. Then, some illustrative results on the generation of oblique waves in the new ECN offshore wave tank are given, comparing the standard snake's principle, and Dalrymple's method. The objective of this research is to investigate both in time and in space the usable test area in a our multi-directional wave tank, for given required sea states.

Introduction

Unlike other methods more commonly used in hydrodynamics such as the BEM, the spectral method is a *global* method in which the solution is expressed in terms of basis functions defined in the whole physical domain. When basis functions are orthogonal, the convergence of the solution is faster than any integer power of the number of unknowns, a behavior usually referred to as 'spectral convergence'. The counterpart of this very interesting characteristic is mainly found in the limitation to simple geometrical domains in which the set of basis functions is defined. Among others, examples of spectral methods applied to free surface flows include Dommermuth & Yue (1987) and Chern *et al* (1999). In applications to inviscid free surface flows, it is possible for certain geometries to find a set of orthogonal basis functions satisfying Laplace's equations, so that the coefficients of the spectral expansion are determined through boundary conditions only. In this spirit, some results concerning non linear sloshing in fixed or moving 2D and 3D tanks were presented at the previous workshop (Ferrant & 2001). The interaction of 2D nonlinear waves modeled by a non linear spectral formulation, with a 3D structure was further presented in Ferrant, Le Touzé & Pelletier (2001). Agnon & Bingham (1999) proposed a method to eliminate the limitation to fixed boundaries, by introducing the concept of an additional potential satisfying the non-homogeneous boundary conditions, while modified free surface conditions are accounted for by the usual spectral expansion. They solved the 2D linearized wave generation problem with an explicit analytical expression for the additional potential limited to the case of a piston wave maker.
In the present paper, this superposition scheme is extended to three dimensions and to arbitrary segmented wave maker configurations, with the additional potential represented by a spectral expansion as well, while boundary conditions on the free surface and on the wave maker are modeled up to second order with respect to the wave steepness and to the wave maker excursion respectively.
This numerical tool is intended to be used for modeling the wave generation and propagation processes in the new ECN offshore wave basin (50mx30mx5m) , equipped with a 48-flap wave maker on one of the 30m sides. Existing theoretical frames for determining paddle motions include the simple snake's principle first formulated by Biesel (1954) and Dalrymple's theory (1989) in which reflections on lateral boundaries are accounted for to obtain the prescribed wave amplitude at a given distance in the basin. More elaborated methods allow the wave amplitude to be optimized over a certain area in the basin, see Boudet & Pérois (2001). However, all these models are based on first order frequency domain theory. With the present model, we will be able to obtain new and valuable indications on the behaviour of the wave tank.

Linear Spectral Modelization

In this section, we consider a three-dimensional tank of water depth h, width L_y and length L_x, partially filled with an inviscid fluid. Under the potential-flow theory assumption, the governing equation for the unknown velocity potential $\phi(\mathbf{M}(x,y,z),t)$ in the whole fluid domain D is Laplace's equation:

$$\Delta\phi(\mathbf{M},t) = 0 \qquad , \qquad (\mathbf{M} \in D) \tag{1}$$

*abstract proposed for presentation at the $17^{th} WWWFB, Cambridge, UK, 14-17 April 2002$

On the tank right & side walls and bottom, the potential ϕ has to satisfy homogeneous Neumann conditions ; and on the left wall, the following linearized Neumann condition :

$$\frac{\partial \phi}{\partial x}(\mathbf{M},t) = U_{wm}(y,z,t) \qquad , \qquad (x=0) \tag{2}$$

where $U_{wm}(y,z,t)$ is the instantaneous velocity of the wavemaker.

Initially the fluid is at rest. We also suppose the free surface to be single-valued and represented at every time by $z=\eta(x,y,t)$. Thus, the linearized nondimensional kinematic and dynamic conditions at the free surface are formulated as follows:

$$\frac{\partial \eta}{\partial t}(\mathbf{M},t) = \frac{\partial \phi}{\partial z} \qquad , \qquad (z=0) \tag{3}$$

$$\frac{\partial \phi}{\partial t}(\mathbf{M},t) = -\eta - \nu(x)\phi \qquad , \qquad (z=0) \tag{4}$$

where $\nu(x)$ is a damping coefficient used to avoid reflections on the right wall of the tank.

Since, we are willing to expand the potential ϕ in series of natural modes of the tank, we are a priori limited to a geometry fixed in time, whereas we want to have a wavemaker on the left wall of the tank. To get rid of that limitation we will here do the superposition of two potentials, which was first proposed by [4] :

$$\phi(\mathbf{M},t) = \phi_{tank}(\mathbf{M},t) + \phi_{wm}(\mathbf{M},t) \qquad , \qquad (\mathbf{M} \in D) \tag{5}$$

where ϕ_{tank} is the spectral potential in the fixed-geometry tank with its free surface, and ϕ_{wm} an additional potential accounting for the wavemaker but not the free surface, and that is further described hereafter. Therefore, ϕ_{tank} satisfies the equations (1), (3) & (4), and homogeneous Neumann conditions on the tank walls and bottom ; and ϕ_{wm} satisfies the equations (1) & (2), and homogeneous Neumann conditions on the tank right wall and bottom. By solving first the wavemaker contribution, we obtain free surface forcing terms quantities allowing us to solve for the fixed-tank part of the potential.

In order to preserve the accuracy and exponential-convergence properties of our spectral method, we found it interesting to describe also the additional potential through a spectral formulation. We apply therefore the same kind of spectral resolution to our wavemaker boundary value problem as to the fixed-geometry tank boundary value problem. Thus, the two spectral potentials can be expressed as such :

$$\phi_{tank}(\mathbf{M},t) = \sum_{m=0}^{N_{x\phi_{tank}}} \sum_{n=0}^{N_{y\phi_{tank}}} a_{mn}(t) \cos(\overrightarrow{k_{mn}}.\overrightarrow{x}) \frac{\cosh(k_{mn}(z+1))}{\cosh(k_{mn})} \qquad , \qquad (\mathbf{M} \in D) \tag{6}$$

$$\phi_{wm}(\mathbf{M},t) = \sum_{M=0}^{N_{x\phi_{wm}}} \sum_{N=0}^{N_{y\phi_{wm}}} A_{MN}(t) \cos(\overrightarrow{K_{MN}}.\overrightarrow{z}) \frac{\cosh(K_{MN}(-x+4))}{\cosh(4K_{MN})} \qquad , \qquad (\mathbf{M} \in D_{wm}) \tag{7}$$

where $\overrightarrow{k_{mn}} = (m\pi/L_x, n\pi/L_y)$ & $\overrightarrow{K_{MN}} = ((2M-1)\pi/4, N\pi/L_y)$ and $\overrightarrow{x} = (x,y)$ & $\overrightarrow{z} = (z+1,y)$; $N_{\phi_{tank}} = N_{\phi_{xtank}} * N_{\phi_{ytank}}$ and $N_{\phi_{wm}} = N_{\phi_{xwm}} * N_{\phi_{ywm}}$ are the numbers of modes kept. Due to the symmetry on the wavemaker, only the odd modes are kept in ϕ_{wm}.

Numerical Resolution

In the two preceding boundary value problems, the only unknowns are the so-called "modal time amplitudes" $a_{mn}(t)$ & $A_{MN}(t)$, and the free-surface elevation η. In both problems, the spectral formulations (6) & (7) satisfy intrinsically Laplace's equation (1) and homogeneous Neumann conditions.

In the wavemaker boundary value problem (equations (1) & (2) in D_{wm}) that we solve first, we discretize the Neumann condition (2) on the wavemaker ($x=0$) at $N_{\phi_{wm}}$ nodes. Then, we do the same at $N_{\phi_{tank}}$ collocation nodes of the free surface ($z=0$) for the fixed-tank boundary value problem.

To update these unknowns, we use a 4^{th}-order Runge-Kutta time-marching scheme. The knowledge of the A_{MN}- & a_{mn}-unknowns at $t+\Delta t$ requires the resolution of two square linear systems. For the wavemaker part, the $N^2_{\phi_{wm}}$ system is assembled from the wavemaker condition (2) taken at the $N_{\phi_{wm}}$ discretization nodes. The system is solved through a LU-decomposition since the matrix is time-independent. For the fixed-tank part then, using the forcing terms quantities obtained from ϕ_{wm}, we assemble a $N^2_{\phi_{tank}}$ square linear system from the free-surface dynamic condition (4) taken at the $N_{\phi_{tank}}$ free-surface collocation nodes. The hyperbolic cosine terms vanishing at ($z=0$) in the expression of ϕ_{tank} (6), this second linear system is solved by means of Fast Cosine Fourier Transforms.

Second-Order Modelization

At the second-order, the potential is the sum of a first-order potential $\phi_1 = \phi_{1tank} + \phi_{1wm}$, computed as explained in the preceding section, and a second-order potential ϕ_2. The same way the other unknown, the free-surface elevation, is decomposed into the sum of two components : $\eta = \eta_1 + \eta_2$. The second-order potential satisfies homogeneous Neumann conditions on the tank side & right walls and bottom ; in addition, the two unknwons ϕ_2 & η_2 verify the following set of equations:

$$\Delta\phi_2(\mathbf{M},t) = 0 \quad , \quad (\mathbf{M} \in D) \tag{8}$$

$$\frac{\partial\phi_2}{\partial x}(\mathbf{M},t) = -X_{wm}(y,z,t) * \frac{\partial^2\phi_1}{\partial x^2} \quad , \quad (x=0) \tag{9}$$

$$\frac{\partial\eta_2}{\partial t}(\mathbf{M},t) = \frac{\partial\phi_2}{\partial z} - \frac{\partial\phi_1}{\partial x}\frac{\partial\eta_1}{\partial x} - \frac{\partial\phi_1}{\partial y}\frac{\partial\eta_1}{\partial y} - \eta_1\left(\frac{\partial^2\phi_1}{\partial x^2} + \frac{\partial^2\phi_1}{\partial y^2}\right) \quad , \quad (z=0) \tag{10}$$

$$\frac{\partial\phi_2}{\partial t}(\mathbf{M},t) = -\eta_2 - \frac{1}{2}\left|\nabla\phi_1\right|^2 - \eta_1\frac{\partial^2\phi_1}{\partial z\partial t} - \nu(x)\phi_2 \quad , \quad (z=0) \tag{11}$$

In order to solve this set of equations, we do the same superposition as for the first order:

$$\phi_2(\mathbf{M},t) = \phi_{2tank}(\mathbf{M},t) + \phi_{2wm}(\mathbf{M},t) \quad , \quad (\mathbf{M} \in D) \tag{12}$$

Thus, we also have to solve first an additional boundary value problem (equations (8), (9) and homogeneous Neumann conditions) to obtain ϕ_{2wm}, and then the fixed-tank boundary value problem (equations (8), (10), (11) and homogeneous Neumann conditions) to get ϕ_{2tank} and η_2.

Some preliminary results

Our second order spectral model has been run for modeling the generation of oblique regular waves in ECN's wave tank. The wave period is T=1.8 s, and waves propagate at an angle of 20 degrees from the

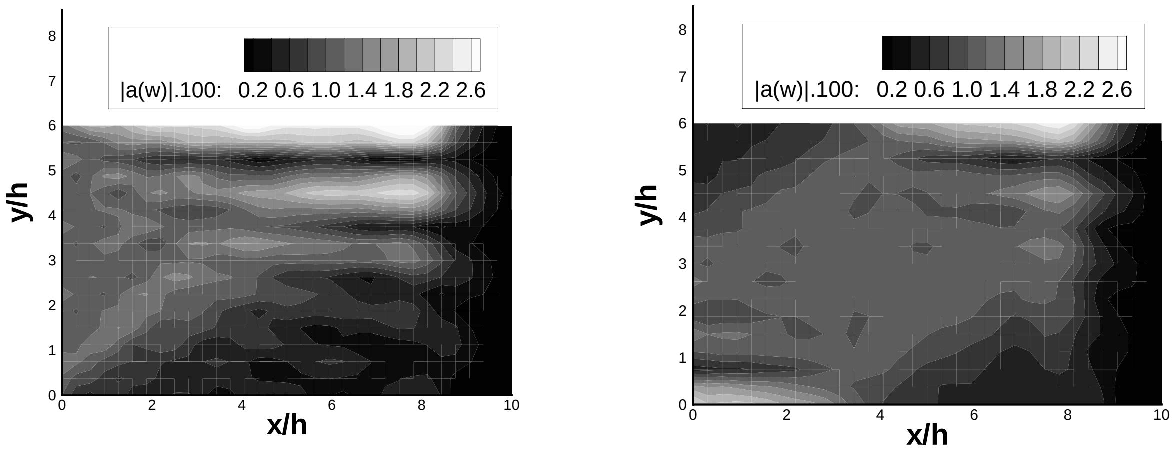

Figure 1: Steady state first order wave amplitudes. Left: Snake's principle. Right: Dalrymple's method

main axis. Both the snake's principle and Dalrymple's method have been tested. In figure 1, we compare the steady state first order wave amplitudes obtained in the tank. These plots have been obtained by applying a moving window Fourier analysis to the unsteady wave amplitude. These results agree with those obtained with a frequency domain first order theory, and illustrate the wider usable zone obtained with Dalrymple's method. This is confirmed by figure 2, giving 3D views of the linear wave fields, observed at t=19T. In figure 3, we give time series of first and second order wave elevations observed at x=17.5m from the wave maker, in the vertical plane of symmetry of the tank, for both types of wave maker control.The second order signal appears to reach a regular steady-state quicker with Dalrymple's control than with the snake's method. This behavior will be further analysed with comments presented at the workshop.

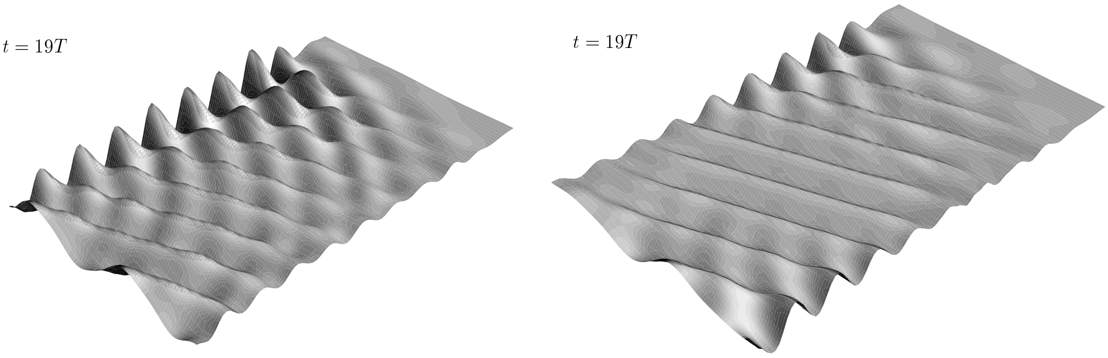

Figure 2: 3D Linear wave fields, t=19T. Left:Snake's principle. Right: Dalrymple's method

Conclusion

A new spectral formulation for the simulation of the generation and propagation of multi-directional waves in a 3D tank has been presented.

The method exhibits the usual performances of spectral schemes, with respect to accuracy and rate of convergence. The effectiveness of the model is illustrated by simulating the generation and propagation of directional waves by a snake wave maker in a 3D tank, using different types of wave maker motion. Future work in this direction includes a better approximation of the physical absorbing beach by the absorbing layer used in the numerical model, and a thorough investigation of the actual usable areas in the tank, with respect to objective sea states.

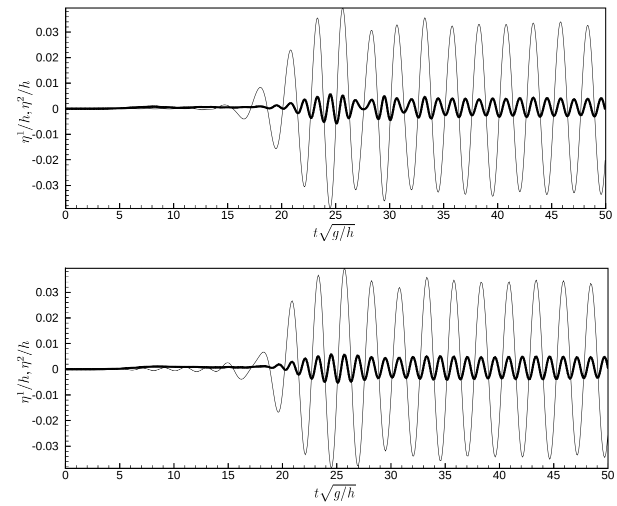

Figure 3: Time series of first- and second-order water elevations at ($x = 0.35 * L_x$, $y = 0.5 * L_y$) (top: Dalrymple, bottom: snake)

References

[1] D.G. Dommermuth & D.K.P. Yue, "A high-order spectral method for the study of nonlinear gravity waves", *J. Fluid Mech.* **184**, 267-288, (1987).

[2] M.J. Chern, A.G.L. Borthwick & R. Eatock-Taylor, "A pseudospectral σ-transformation model of $2D$ nonlinear waves", *J. Fluids and Struct.* **13**, 607-630, (1999).

[3] P. Ferrant & D. Le Touzé, "Simulation of sloshing waves in a $3D$ tank based on a pseudospectral method", *Proc. 16^{th} Int. Workshop on Water Waves and Floating Bodies*, Hiroshima, Japan, (2001).

[4] Y. Agnon, H.B. Bingham , "A non-periodic spectral method with applications to non linear water waves", *Eur. J. Mech. B/ Fluids*, **18**, 527-534, (1999).

[5] P. Ferrant, D. Le Touzé & K. Pelletier, "Non-Linear Time Domain Models for Irregular Wave Diffraction about Offshore Structures", *Proceedings ECCOMAS Computational Fluid Dynamics Conference*, Swansea, Wales, (2001).

[6] F. Biesel , 'Wave machines', *Proceedings of the First Conference on Ships and Waves*, (1954).

[7] R.A. Dalrymple , 'Directional Wavemaker Theory with Sidewall Reflection', *Journal of Hydraulic Research*, **27**, n1, 23-34., (1989).

[8] L. Boudet, J.P. Pérois , 'Nouvelles techniques de pilotage d'un batteur segmenté pour la génération de houle oblique ', *Comptes Rendus des Huitièmes Journées de l'Hydrodynamique*, Nantes, ISSN 1161-1847, (2001) (in French).

Discussion Sheet

Abstract Title :	Second-Order Spectral Simulation of Directional Wave Generation and Propagation in a 3D Tank		
(Or) Proceedings Paper No. :	26	***Page :***	099
First Author :	Le Tousé, D.		
Discusser :	Bernard Molin		

Questions / Comments :

I wonder which damping condition you apply to the second-order waves at the far end of the tank. As the wavemaker is switched on, a long wave is generated, which is second-order in the wave amplitude and which propagates at celerity $\sqrt{gh}$. Another long wave travels together with the wave front. In physical basins, traditional beaches are totally ineffective in absorbing these long waves. In my opinion, when first and second-order wave fields are separated, it is more correct to apply no absorbing condition at all to the second-order waves : long waves get reflected ; as for the double frequency free waves, it takes them a long time to reach the far end of the tank, so it is not really a problem that they get reflected.

Author's Reply :
(If Available)

Since our aim is actually more to reproduce more precisely what happens in a physical wavetank, such as our new ECN facility, rather than perfectly absorb the wave train, this remark appeared very interesting to us. Indeed, implemented as was, a second-order absorption was effective. Thus, in order to verify its impact on the second-order long waves described above, we run a case with and without this absorption being active, and we then compared. It appeared to be easier for us to look to the long and fast wave mentioned in the comment, of theoretical celerity $\sqrt{gh}$ and that propagates ahead of the wavefront, since it propagates alone, rather than the one propagating behind along with the wavefront.
We chose to do a simple 2D regular-wave simulation in a numerical tank similar to our physical one (the one used (and described) in the paper as well, but in 3D), where a parabolic absorbing zone applies from 0.8Lx/h to Lx, at first order in both cases and at second-order in one case. Please refer to the paper itself for the domain dimensions and the description of the numerical absorption implementation.
The wave generated has a nondimensional pulsation of 2.5. The figure below shows the second-order water elevation at a probe located at the start of the absorbing zone (x/h=0.8Lx/h) in the two cases. The bottom plot is a zoom of the top one in the time area where the $\sqrt{gh}$ -celerity long wave is forecasted to reach the probe, first on its incoming way (first dashed vertical line), and then on its way back after reflection (second dashed vertical line). One can first notice that the time when the long wave first reaches the probe actually matches the theory. Second, the comparison clearly shows that having a second-order absorption actually damps this long wave.

Therefore, provided that one works with times prior to the reflected double frequency free waves reaching the usable area of the basin, removing our second-order absorption condition actually leads to a closer reproducing of the physical wave tank generation and propagation process.
Finally, it shall be mentioned that substantial advances have been made since the time when the paper in the proceedings was written (where figure 3 is not correct, by the way). For further results and analysis, please refer to the proceedings of the ISOPE 2002 Conference to be held in Japan early June.